Chemical Geology 621 (2023) 121356

Contents lists available at ScienceDirect

Chemical Geology

journal homepage: www.elsevier.com/locate/chemgeo

Oxygen isotopic composition of Paleoproterozoic seawater revealed by clumped isotope analysis of dolomite, Vempalle Formation, Cuddapah, India

Sanchita Banerjee [a], Prosenjit Ghosh [a,b,*], Yogaraj Banerjee [a], Robert Riding [c]

[a] Centre for Earth Sciences, Indian Institute of Science, Bangalore, India
[b] Divecha Centre for Climate Change, Indian Institute of Science, Bangalore, India
[c] Department of Earth and Planetary Sciences, University of Tennessee, Knoxville, USA

ARTICLE INFO

Editor: Michael E. Boettcher

Keywords:
Palaeoproterozoic
Vempalle
Dolomite
Clumped isotope thermometry
Seawater composition
Diagenesis.

ABSTRACT

The Paleoproterozoic (~2.0–1.9 Ga) Vempalle Formation, in the south-western part of the Cuddapah Basin, is a well-studied Paleoproterozoic succession. Detailed descriptions of sedimentological features, micro-textures, and isotopic compositions of dolomite in the stromatolites and associated lithologies suggest that the succession was deposited on a carbonate ramp. Early burial diagenesis of the dolomite modified the original isotopic signatures. Nonetheless, here we discern evidence for two distinct depositional events based on clumped isotopic signatures preserved within dolomitic stromatolite and the underlying dolomite mud. Dolomitic muds within cherty precipitate record original thermometry signatures from these rocks. Clumped isotope analyses suggest that the lowest temperature of the Paleoproterozoic seawater was 21.8 ± 2 °C, and that its isotopic composition ($\delta^{18}O_{VSMOW}$) during dolomite precipitation at equilibrium was −9.6 ± 0.1‰, which is lighter than that of present-day ocean water. The overlying stromatolitic dolomite exhibits a temperature range of 70.7–109.8 °C, reflecting late-stage diagenetic processes and hydrothermal activity. Hydrothermal fluids were isotopically enriched (up to 4.9‰) suggesting their mantle origin and interaction with evaporative seawater. We evaluated the degree of water-rock interaction with water of heavier isotopic composition that was responsible for the precipitation of late phase dolomite found in the strata overlying carbonate mud.

1. Introduction

Proterozoic seawater differed from the modern ocean with respect to its temperature and pCO_2, and had an Mg/Ca ratio that favored the deposition of microbial dolomite. This study focuses on the Paleoproterozoic Vempalle Formation, Cuddapah Basin, India which displays a sedimentary record having well-preserved dolomitic microbial carbonates (Riding and Sharma, 1998; Khelen et al., 2017; Patranabis-Deb et al., 2018; Banerjee et al., 2019; Panja et al., 2019). Our goal is interpretation of the depositional environment of these well-preserved precipitates using stable and clumped isotope analysis of dolomite minerals present in these lithologies. Sedimentary features, soft-sedimentary deformation structures (e.g., rip-up clasts, *syn*-sedimentary breccia, mud-cracks, convolute bedding) and geochronological data indicate shallow-water depositional environments for these sediments in a rifted basin ~1900–2000 Ma ago. Petrographic studies of the dolomitic carbonate units reveal the presence of microbial structures together with abiogenic carbonates with signatures of early diagenesis. The fine grained microbial dolomitic carbonates and presence of filamentous structures (Riding and Sharma, 1998; Banerjee et al., 2019) indicate good preservation. Previous geochemical studies based on stable isotopic and rare earth element composition suggest that the carbonate units were deposited in shallow marine environments and underwent *syn*-sedimentary dolomitization (Khelen et al., 2017; Patranabis-Deb et al., 2018; Banerjee et al., 2019).

Clumped isotope thermometry (Ghosh et al., 2006) is used here to evaluate physical factors during carbonate precipitation (primarily temperature and water composition). Previous studies (Frantz et al., 2014; Petryshyn et al., 2015) of clumped isotope thermometry for lacustrine stromatolites showed that microbially induced carbonates are potential archives for paleotemperature reconstruction and are able to record seasonal-scale temperature variations. Carbonic anhydrase

* Corresponding author at: Centre for Earth Sciences, Indian Institute of Science, Bangalore, India.
E-mail address: pghosh@iisc.ac.in (P. Ghosh).

https://doi.org/10.1016/j.chemgeo.2023.121356
Received 15 February 2022; Received in revised form 2 January 2023; Accepted 29 January 2023
Available online 1 February 2023

(Thaler et al., 2016; Thaler et al., 2020) that assisted precipitation of the microbial carbonate allows the water composition to be deciphered due to attainment of equilibrium during carbonate deposition without any 'vital effect'. Thus, fundamental questions concerning the isotopic composition of the Paleoproterozoic hydrosphere can be assessed from this relatively well-preserved carbonate.

1.1. Materials

We examined carbonate mud (micrite) and three overlying stromatolite deposits with distinctive morphotypes in the Vempalle Formation of the Paleoproterozoic Cuddapah Basin. Fresh specimens of carbonate mud and stromatolites collected from a road-cut section in the Vempalle Formation near Pulivendla (N 14°26 E 78°21), Andhra Pradesh, India, were examined for stable and clumped isotopes. The sampling location and their position in the stratigraphic succession are shown in Fig. 1.

1.2. Dolomite mud and stromatolite morphotypes

Carbonate mud layers intercalated with chert and intraclasts are abundant in the lower part of the succession. The lime mud layers are massive micritic dolomite encased in chert. Polygonal mud cracks that are abundant on the bedding planes denote sub-aerial exposure following deposition. Stromatolites collected from the lower part of succession, overlying the lime mud layer, are morphologically well preserved and mostly micritic to micro-sparitic in texture and devoid of obvious replacement features as revealed from microscopic investigation. Based on macroscopic curvature and layer thickness (Fig. S1), as well as microscopic features, three stromatolite morphotypes can be distinguished.

Type I. Large dome shaped stromatolites characterized by thick, alternating light gray and dark black bands that range from 0.3 to 0.8 mm in thickness (Fig. S2). These coarsely layered stromatolites commonly form expanding branched domes (Fig. S2.c). Microscopically the stromatolite fabric is heterolithic. Large acicular radiating dolomite crystals resembling spherulitic texture are prominent in the dark-colored layers (Fig. S2, e, f). Light colored bands are comparatively homogeneous and micritic. In places, microscale bandings are also observed within the layers (Fig. S2, g).

Type II. Finely layered columnar stromatolites exhibit dark and light macroscale alternating bands resembling those of Type I, but thinner (0.1 to 0.2 mm). The dark layers are thinner than the lighter ones and have low relief, displaying comparatively uniform columns (Fig. S3). Cross cutting laminae indicate *syn*-sedimentary scour (Fig. S3.c). Thin sections show alternating micritic and micro-sparite layers (Fig. S3.e) and patchy crystalline dolomite (Fig. S3.f).

Type III. Microdigitate stromatolite is macroscopically very different from the other stromatolites. It exhibits intergrowth of light gray layers (Fig. S4) with mostly dark colored bands, unlike the prominent alternations of bands in Type I and Type II stromatolite. Dark colored acicular dolomite grains are abundant. The intergrown nature of the layered structures is also visible at microscale within the layers (Fig. S4.e). In SEM images, prominent euhedral crystals within microbial carbonate matrix were probably precipitated during late phase intrusion of hydrothermal fluids (Fig. S4.h).

1.3. Other sedimentary structures present in the Vempalle Formation

The lithological and sedimentary structures in the Vempalle Formation (Fig. S5.a and b), along with the stromatolites, are indicative of high energy shallow marine conditions. Lithotypes present in the sequence, in order of decreasing abundance, are carbonate mudstone, intraclasts, oolite, flat-pebble conglomerate, crystal crusts and red-beds. Shrinkage- cracks on the surface of carbonate mud (Fig. S7.a) imply subaerial exposure. Gray colored carbonate mud is abundant in the lower part of the sequence, and a single unit of red colored carbonate mud was observed containing irregular-shaped reduced patches (Fig. S6. d). Ripple marks on the carbonate mud (Fig. S8.a) indicate wave and current action. Evidence of storm events is very common throughout the section. Flat pebble conglomerates in the basal part, and intraclasts within the oolitic layers, indicate high energy conditions during

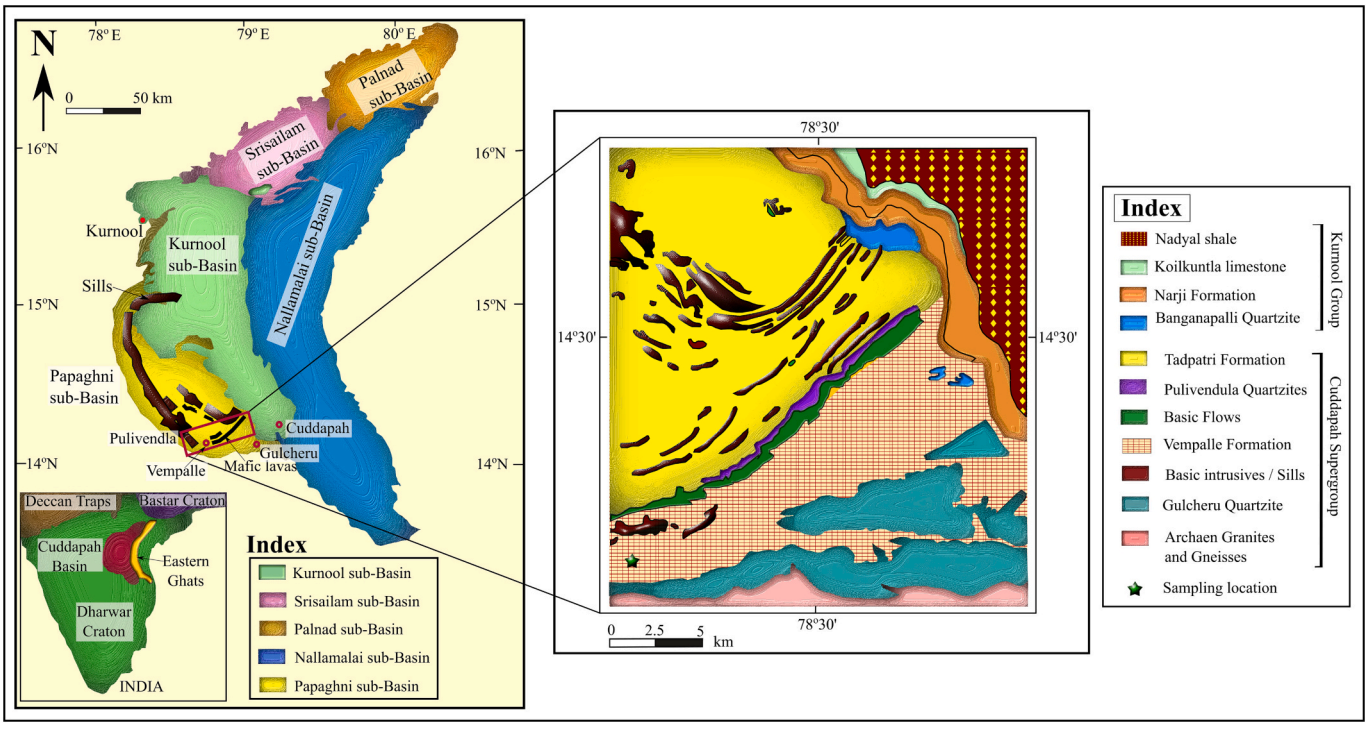

Fig. 1. (a) Geological map of the Proterozoic Cuddapah Basin, India (after Singh et al., 2018). (b) Geological map of the study area showing sampling location (c) Lithologies of the Vempalle Formation showing the stratigraphic position of specimens used in this study.

deposition The carbonate mud flakes are locally arranged in 'pack of cards' structure (Fig. S7.b), and a conglomerate bed consists of rip-clasts formed during *syn*-sedimentary deformation (Fig. S7.c). Flame structures and incipient molar tooth structure (Fig. S6.c) are also evidence of soft sediment deformation. Large oncoids in adjacent strata appear to be nucleated on large carbonate mud flakes (Fig. S6.a and b). Secondary chert replacement of fine agglutinated stromatolites is common throughout the sequence (Fig. S5.a).

2. Methods

Analyses of clumped and stable isotopes were undertaken to evaluate the temperature of formation and the nature of the precipitating fluids. Experiments were performed following the break-seal method (Fosu et al., 2019) and floating-boat method (Rangarajan et al., 2021) of acid digestion.

2.1. X-ray Diffraction analysis

Small fragments of carbonate mud, and of the three different stromatolite morphotypes, collected from the outcrop were polished and powdered using a microdrill for X-ray diffraction analysis in a Rigaku X-ray Diffractometer in the Department of Physics, IISc (Bangalore, India) for 2θ range of 5–90° (Supporting data 1 – two theta). XRD analyses identified dolomite as the carbonate phase present in both the stromatolite and lime mud samples. Carbonate mud samples contained significant amounts of chert along with dolomite.

2.2. Stable isotope analysis

Bulk ($\delta^{13}C_{VPDB}$ and $\delta^{18}O_{VPDB}$) isotope compositions of the stromatolitic dolomites were measured in continuous flow mode following the floating boat method using Gas bench II peripheral connected with IRMS MAT 253. The procedure is described in Rangarajan et al. (2021) where sample powder was reacted at 70 °C for >12 h. Polished sections of layered stromatolites were drilled at 2–3 mm spatial resolution, depending on the layer thickness of the light and dark colored bands, using a micro-drill. For analysis, powdered dolomite samples (~0.7 mg) were loaded into glass boats and placed inside exetainer vials containing ~0.1 ml of concentrated phosphoric acid (>104%). Capped exetainer vials, with sample powder and acid, placed in two compartments were flushed with He (99.99%) at 100 ml/min to remove any air present in the headspace. The powder within the He-flushed vials was reacted with the acid by tilting the boat suspended on the acid, and placed into the bath maintained at constant temperature of 70 °C. The CO_2 evolved during reaction inside the exetainer vials was cleaned using a gas chromatography column purged with a stream of continuous He-flow designed for Gas Bench II (Thermo Finnigan) and analyzed for $\delta^{13}C_{VPDB}$ and $\delta^{18}O_{VPDB}$ using a Thermo MAT 253 isotope ratio mass spectrometer in the Stable Isotope Laboratory, IISc (Bangalore, India).

2.3. Clumped isotope analysis of samples

Clumped isotope analyses of dolomite powders taken from the lime-mud and stromatolite samples were undertaken following the procedure described in the break-seal method (Fosu et al., 2019). 10–12 mg of dolomite powder was drilled from each of the stromatolite and lime mud layers present in the hand specimens. Dolomite powder collected for each analysis was loaded within a narrow Pyrex tube and placed within a wider Pyrex tube containing 1 ml phosphoric acid (>104%, Merck, Darmstadt, Germany). Pyrex tubes with sample powder and acid were evacuated through a glass line using a rotary-pump to reach the background pressure of 10^{-3} mbar. The evacuation was followed by sealing the Pyrex tubes using an oxy-acetylene flame to isolate the entire system from the surroundings. Powdered dolomite samples were then reacted with the phosphoric acid at 25 °C and allowed to react within a water bath for >72 h (Pramanik et al., 2020). MAR J1 and OMC were analyzed as reference materials along with dolomite standard (CO3-dolomite). MAR J1 and OMC carbonate powders were reacted following the same protocol for 18 h. CO3-dolomite reference carbonate was analyzed intermittently to assess the analytical reproducibility for dolomite samples. CO_2 generated upon completion of reaction from each of these samples was extracted cryogenically using liquid N_2 into an ampoule in the presence of a moisture trap maintained at −80 °C using an ethanol+liquid N_2 slurry. Trapped CO_2 was entrained through a Porapak-Q GC column (2 m length, 1/8″ diameter, 80/100 mesh) maintained at 25 °C, using He as the carrier gas to minimize isobaric interference from contaminants. The GC column was heated at 150 °C intermittently to remove contaminants accumulated through time. Pure CO_2 from dolomite and calcite reference materials was introduced to the dual inlet peripheral of a Thermo MAT 253 isotope ratio mass spectrometer with Linde CO_2 acting as the working gas. The measurement was continued for 100 cycles. Remaining CO_2 after completion of each analysis was retrieved in a quartz tubes (high purity) using liquid N_2 and sealed. The tube is then heated at 1000 °C inside a muffle furnace to generate heated gas or CO_2 which is stochastic. The CO_2 sample was extracted and analyzed following the protocol described in Fosu et al. (2019). Multiple head gases with variable composition were used to establish the non-linearity correction factor. The major ion beam intensity during most of the clumped isotope analyses was maintained in the range 10,000-12,000 mV. Each of the analytical sessions constitutes a sequence containing 10 acquisitions with alternate cycles of CO_2 from sample and reference bellow (working gas). Linde CO_2 (Germany) was used as the working gas for the measurement purpose, which was independently calibrated with primary reference carbonate NBS-19 and assigned $\delta^{13}C_{VPDB}$ and $\delta^{18}O_{VPDB}$ values of −3.92‰ and 25.58‰ respectively.

3. Data reduction process

3.1. Stable and clumped isotope data

The $\delta^{13}C_{VPDB}$ and $\delta^{18}O_{VPDB}$ values of the Vempalle dolomite samples measured using Gas Bench II were corrected by anchoring the values to internal laboratory standard MAR J1 calcite, which was independently calibrated with primary reference material NBS-19 (Ghosh et al., 2005). The internal reference calcite was analyzed intermittently during sample runs.

The measured raw Δ_{47} values were corrected to represent the absolute reference frame (Dennis et al., 2011) for the values, using the parameters provided in Daëron et al., 2016. CO_2 samples equilibrated at 25 °C and heated at 1000 °C were analyzed to construct the equilibrated gas line (EGL) slope and intercept using the weighted regression method. Δ_{47} values of MAR J1 and OMC were used to construct the secondary reference frame for the conversion of data in the absolute reference frame (ARF). The accepted values of Δ_{47} for MAR J1 and OMC used for data correction are 0.395 ± 0.02‰ and 0.587 ± 0.02‰ respectively (Fosu et al., 2019). Clumped temperature was evaluated using the available calibration equation for dolomite clumped isotope thermometry by Bonifacie et al. (2017) and updated by Müller et al. (2019). Both the experimental observations used the acid drip method (Kiel device) and the acid digestion temperatures were 90 °C and 70 °C respectively (Table 1). Since in the present study all the experimental data are based on CO_2 generated at 25 °C with prolonged reaction time, the resultant Δ_{47} values were corrected for an acid fractionation offset of 0.063‰ for 90 °C and 0.03‰ for 70 °C (Pramanik et al., 2020). Near stoichiometric CO3-dolomite ($Ca_{0.49}Mg_{0.51}(CO_3)$) was reacted at three different temperatures using the break-seal method to estimate the correction factor required for the conversion of Δ_{47} values reported at 25 °C to 70 °C and 90 °C. Temperature estimates using the equation provided in Müller et al. (2019) were slightly lower than the values obtained by using the equation proposed in Bonifacie et al. (2017).

The $\delta^{18}O_{VPDB}$ values for dolomites obtained during clumped isotope

Table 1
Isotopic composition ($\delta^{13}C_{VPDB}$, $\delta^{18}O_{VPDB}$, $\delta^{18}O_{VSMOW}$, Δ_{47} in ‰), clumped isotope-based temperature (°C), oxygen isotopic composition of water($\delta^{18}O_{VSMOW}$), and water-rock ratio (W/R) reported from the dolomite mud and three different types of stromatolite samples of the Vempalle Formation (VF). Clumped isotope temperature is evaluated for dolomite using the equation proposed by Bonifacie et al. (2017) and Müller et al. (2019). The water isotope composition is evaluated using the oxygen isotope fractionation equation proposed by Horita (2014) and Müller et al. (2019).

Sample ID	Description	$\delta^{13}C$ (‰ VPDB)	$\delta^{18}O$ (‰ VPDB)	$\delta^{18}O$ (‰ VSMOW)	Δ_{47} ARF	TEMPERATURE (°C) Bonifacie et al., 2017 corrected for acid fractionation at 90 °C	Müller et al., 2019 Corrected for acid fractionation factor at 70 °C	$\delta^{18}O$water (in ‰ VSMOW) (Vasconcelos et al., 2005)	$\delta^{18}O$water (in ‰ VSMOW) (Müller et al., 2019)	$\delta^{18}O$water (in ‰ VSMOW) (Horita, 2014)	water fraction	W/R
VF/STR/ TP1_A	Type I stromatolite, VF	−0.17	−8.05	22.62	0.48	104.81	103.37	2.86	3.63	3.36	0.92	12.30
VF/STR/ TP1_B	Type I stromatolite,VF	−0.1	−7.68	23.01	0.52	81.86	80.66	0.68	1.21	0.81	0.75	2.95
VF/STR/ TP1_C	Type I stromatolite,VF	−0.13	−7.94	22.74	0.47	111.28	109.77	3.61	4.45	4.22	0.98	Infinite
VF/STR/ TP1_D	Type I stromatolite,VF	−0.16	−7.97	22.7	0.48	104.81	103.37	2.93	3.71	3.44	0.93	13.34
VF/STR/ TP1_E	Type I stromatolite,VF	−0.15	−7.83	22.85	0.54	71.84	70.75	−0.75	−0.35	−0.82	0.63	1.73
VF/STR/ TP2_A	Type II stromatolite, VF	−0.06	−7.52	23.17	0.49	98.66	97.29	2.75	3.46	3.17	0.91	10.25
VF/STR/ TP2_B	Type II stromatolite, VF	−0.01	−7.63	23.05	0.53	76.74	75.60	0.08	0.55	0.11	0.70	2.32
VF/STR/ TP2_C	Type II stromatolite, VF	−0.1	−7.41	23.29	0.51	87.20	85.95	1.59	2.18	1.81	0.82	4.47
VF/STR/ TP2_D	Type II stromatolite, VF	−0.09	−7.47	23.22	0.51	87.20	85.95	1.53	2.11	1.75	0.81	4.33
VF/STR/ TP2_E	Type II stromatolite, VF	−0.06	−7.03	23.68	0.52	81.86	80.66	1.34	1.86	1.46	0.79	3.82
VF/STR/ TP3_A	Type III stromatolite, VF	0.12	−7.25	23.44	0.52	81.86	80.66	1.10	1.63	1.23	0.78	3.47
VF/STR/ TP3_B	Type III stromatolite, VF	0.11	−7.25	23.44	0.48	104.81	103.37	3.66	4.43	4.17	0.98	50.89
VF/STR/ TP3_C	Type III stromatolite, VF	0.05	−7.08	23.63	0.5	92.80	91.49	2.57	3.21	2.88	0.89	8.20
VF/STR/ TP3_D	Type III stromatolite, VF	0.09	−6.98	23.72	0.49	98.66	97.29	3.29	4.00	3.71	0.95	18.46
VF/STR/ TP3_E	Type III stromatolite, VF	0.09	−6.82	23.89	0.51	87.20	85.95	2.18	2.77	2.40	0.86	6.04
VF/CARB MUD_1	Carbonate mud, VF	−0.26	−7.96	22.72	0.64	32.01	31.25	−7.23	−7.44	−8.25	0.12	0.13
VF/CARB MUD_3	Carbonate mud, VF	−0.23	−7.95	22.72	0.62	38.88	38.06	−5.96	−6.05	−6.79	0.22	0.28
VF/CARB MUD_4	Carbonate mud, VF	−0.25	−8.37	22.29	0.67	22.52	21.82	−9.54	−9.94	−10.84	−0.06	−0.06
VF/CARB MUD_5	Carbonate mud, VF	−0.34	−8.53	22.13	0.66	25.58	24.87	−9.07	−9.40	−10.27	−0.02	−0.02

analysis were further used to evaluate $\delta^{18}O_{VSMOW}$ of water assuming a thermodynamic equilibrium condition for precipitation and expressed in the oxygen isotope fractionation equation provided by Horita (2014) and Müller et al. (2019). The water isotopic composition was calculated using the temperature data obtained from Müller et al. (2019) and applying three different available empirical relationships (Vasconcelos et al., 2005, Horita, 2014 and Müller et al., 2019) (Supplementary Table 1). The differences between the predicted water isotopic values are small (within 1‰), however for the purpose of our discussion we adopted the values obtained using the Müller et al. (2019) equation, which are lighter in composition. Moreover, the relationship provided by Müller et al. (2019) is more appropriate covering a large range in temperature (25 °C to 350 °C) for dolomite precipitation and comprehensive with inclusion of previous observation by other workers (Vasconcelos et al., 2005; Horita, 2014.

The water rock ratio was calculated using the minimum and maximum isotopic values of water inferred from Müller et al. (2019). The heavier water of hydrothermal origin is considered as the end member for interaction with pristine dolomite carrying a signature of sea water. The temperature data were calculated using the equation designated for the dolomite (Müller et al., 2019) calibration experiment. The lowest temperature value of 21.8 °C is observed in the present study for dolomite mud encased within cherty layers. Such a temperature estimate for the early Proterozoic ocean is close to estimates using Si^{30} isotope with multiple assumptions (Robert and Chaussidon, 2006).

3.2. Estimation of water rock interaction

The water rock interaction during late phase diagenetic alteration interacting with the hydrothermal fluid was calculated based on the clumped isotope temperature estimates, water isotopic composition predicted from the dolomite mud at equilibrium, and comparison with the overlying stromatolite layers at equilibrium. The Type III stromatolite sample, which records the highest temperature (110 ± 2 °C) and the enriched water oxygen isotopic composition($\delta^{18}O_{VSMOW}$) of 4.45‰, is assumed to represent the end member composition defining the hydrothermal source, generated by the intrusive features such as sills and dykes (Anand et al., 2003; Jaffrés et al., 2007; French et al., 2008; Khelen et al., 2017; Banerjee et al., 2019). The value represents one end member in the spectrum of the observed range (4.45 to 3.63 ‰) of water isotope values deduced from the high temperature dolomites (>100 °C) analyzed in the present study (Table 1). The water isotope composition of −9.94‰ established for the dolomite lime mud, which registered a clumped isotope temperature value of 21.8 ± 2 °C, represents the unaltered Paleoproterozoic ocean water isotopic value and is adopted here as the other end member for modelling purposes. The lighter composition and temperature state are not the same but are close to other studies (Jaffrés et al., 2007; Galili et al., 2019). Based on these end member water isotope compositions, the water-to-rock ratio is calculated using the following equation:

$$\frac{W}{R} = \frac{\frac{\delta^{18}O_{VSMOW(initial\ water)} - \delta^{18}O_{VSMOW(dolomite)}}{\delta^{18}O_{VSMOW(initial-water)} - \delta^{18}O_{VSMOW(altered-water)}}}{1 - \left(\frac{\delta^{18}O_{VSMOW(initial\ water)} - \delta^{18}O_{VSMOW(dolomite)}}{\delta^{18}O_{VSMOW(initial-water)} - \delta^{18}O_{VSMOW(altered-water)}}\right)} \quad (1)$$

where W is the fraction of water involved in alteration, and R is the fraction of dolomite. The process of alteration is visualized invoking a mass balance approach, where hydrothermal fluid with heavier isotopic value is allowed to interact with the portion (fraction) of rock characterized by lighter isotopic composition. The $\delta^{18}O_{VSMOW(dolomite)}$ refers to water composition obtained from the measured temperature and $d^{18}O$ of the dolomite mud. The sea water end-member $\delta^{18}O_{VSMOW(initial\text{-}water)}$ is −9.94‰ and the hydrothermal water is characterized by a $\delta^{18}O_{VSMOW(altered\text{-}water)}$ value of 4.45‰ which is assigned the clumped temperature value of 109.8 °C.

4. Results

Variations in $\delta^{13}C_{VPDB}$ and $\delta^{18}O_{VPDB}$ measured from the different dolomitic facies are shown in Fig. 2 and compared with the values reported from previous studies (Chakrabarti et al., 2014; Khelen et al., 2017; Banerjee et al., 2019). The spectrum of $\delta^{18}O_{VPDB}$ values measured previously by multiple workers was compared with the present study to provide a comprehensive assessment of the variability in composition and its similarity with the present study. Type II finely layered columnar stromatolite exhibits clusters of $\delta^{13}C_{VPDB}$ and $\delta^{18}O_{VPDB}$ values, whereas type I and type III stromatolites show large scatter suggesting admixture of carbonates precipitated from water originating from hydrothermal sources (Supporting data 2). $\delta^{13}C_{VPDB}$ values for type I, II and III stromatolites fall within a narrow range from −0.1 to −0.17‰, −0.1 to −0.01‰ and 0.05 to 0.12‰ respectively. $\delta^{18}O_{VPDB}$ values for type I, type II and type III stromatolites range from −8.05 to −7.03‰, −7.63 to −7.41‰ and − 7.25 to −6.82‰ respectively. $\delta^{13}C_{VPDB}$ and $\delta^{18}O_{VPDB}$ values recorded during the clumped isotope measurement of dolomite mud and stromatolites are also included, together with Gas Bench data of multiple drill spots from the same hand specimens (Fig. 2), where the variation in stable isotopic values with change in the clumped isotope-based temperature estimate are shown by a color gradient.

The data on $\delta^{13}C_{VPDB}$, $\delta^{18}O_{VPDB}$, clumped isotope temperature (°C) and associated water isotope composition ($\delta^{18}O_{VSMOW}$) observed from the clumped isotopic analyses of dolomite mud and stromatolite samples of the Vempalle Formation are displayed in Fig. 3 and Table 1. $\delta^{13}C_{VPDB}$ values for dolomite mud range from −0.23 to −0.34‰. Dolomite mud recorded the lowest temperature in the stratigraphic column studied, ranging 21.8–38.1 °C based on Müller et al. (2019). Clumped isotopic temperatures for type I, type II and type III stromatolites range 70.8–109.8 °C, 75.6–97.3 °C and 80.7–103.4 °C respectively based on Müller et al. (2019). The temperature values show 2 °C excess if the other equation is used (Bonifacie et al., 2017) (Supplementary Table 1).

Oxygen isotope composition of the environmental water was calculated assuming an equilibrium condition for precipitation of dolomite and using the measured $\delta^{18}O$ values of dolomite and the clumped isotope-based temperature estimates. $\delta^{18}O_{VSMOW}$ values for water obtained from dolomite mud range − 9.94 to −6.05‰. Water oxygen isotopic compositions of fluid responsible for the precipitation of dolomite in type I, type II and type III stromatolites range − 0.35 to 4.45‰, 0.55 to 3.46‰ and 1.63 to 4.43‰ respectively (Table 1 and Fig. 4).

5. Discussion

5.1. Stable and clumped isotopic composition variability in dolomite

$\delta^{13}C_{VPDB}$ values reported from the dolomite lime mud and stromatolites inherit the composition of marine water with a scatter denoted by the standard deviation of <0.05‰. Variability of $\delta^{18}O_{VPDB}$ data from different parts of the stromatolite is explained by post depositional changes, which include burial diagenesis and fluid rock interaction. Type III microdigitate stromatolite exhibited maximum enriched $\delta^{18}O_{VPDB}$ values with a scatter, denoted by a standard deviation of 0.2‰, probably caused by late phase burial diagenesis due to involvement of hydrothermal fluid with heavier oxygen isotopic value. The small scatter of $\delta^{13}C_{VPDB}$, $\delta^{18}O_{VPDB}$ and clumped temperature values observed from the dolomite mud suggests a homogeneous and relatively pristine nature of the sediment. Absence of correlation between $\delta^{13}C_{VPDB}$ and $\delta^{18}O_{VPDB}$ ($R^2 = 0.062$), and the narrow range of $\delta^{13}C_{VPDB}$ value for all the specimens, denote limited diagenetic modification but stronger influence of hydrothermal fluid action in an environment dominated by the process of evaporative transformation of the original water composition.

5.2. Late phase alteration and dolomitization of stromatolites

The presence of two different generations of dolomite allows

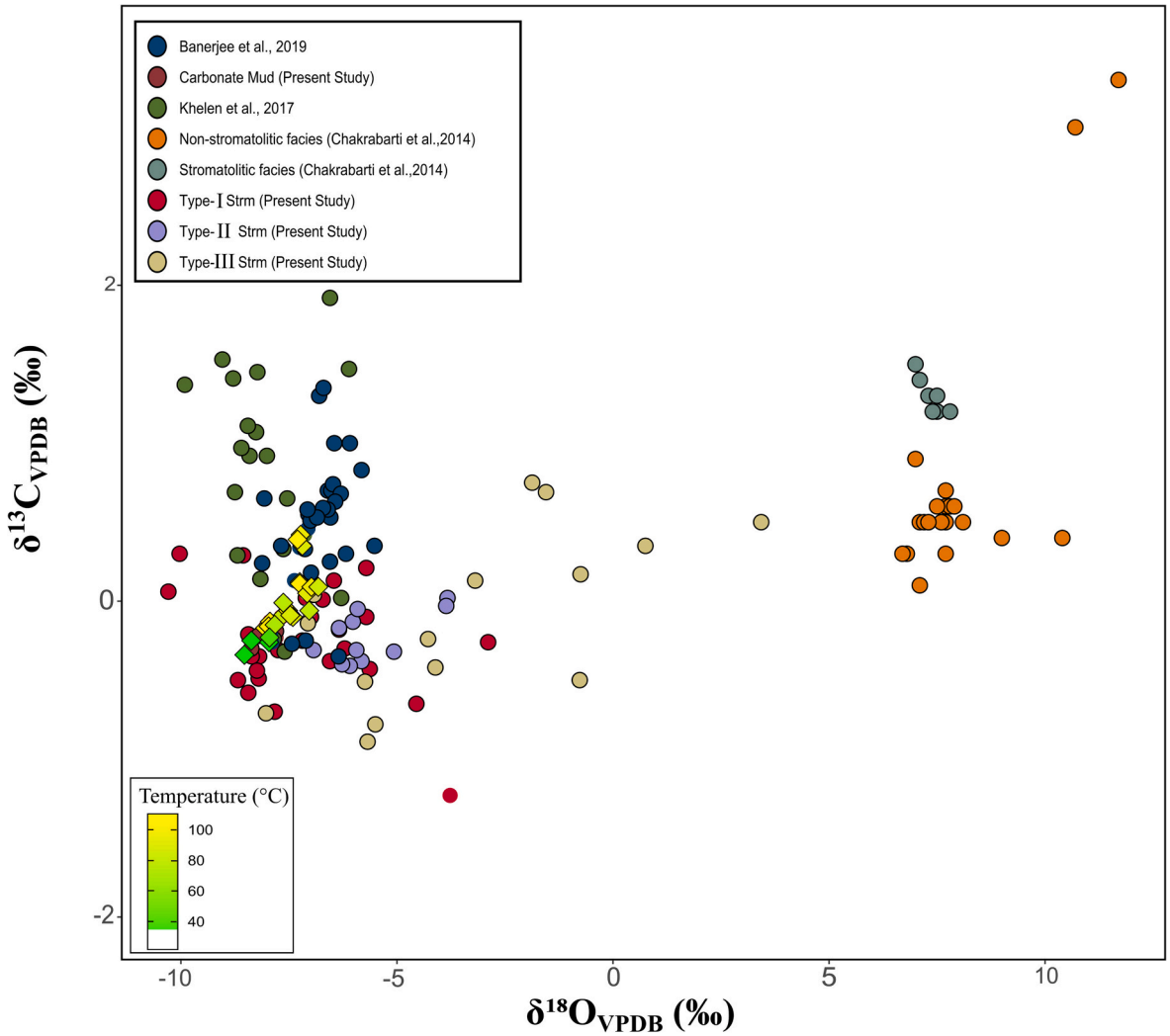

Fig. 2. Variation of $\delta^{13}C_{VPDB}$ and $\delta^{18}O_{VPDB}$ in dolomites from stromatolite and non-stromatolite lithologies in the present study measured using Gas bench II and compared with values from previous studies (Banerjee et al., 2019; 524 Chakrabarti et al., 2014; Khelen et al., 2017). Also plotted are dual inlet measurements of stable isotopes along with clumped temperatures. The data points are shown by diamond symbols, with temperature gradient indicated by shading.

evaluation of the degree of transformation, assuming dolomite mud and type III stromatolite as the primitive and most altered carbonates respectively, in the spectrum of dolomite investigated here. The oxygen isotopic composition of water established using the equation of Horita (2014) deviates from the composition of Müller et al. (2019) by 0.06 to 0.2‰. The equation for fractionation factors proposed in the earlier work (Vasconcelos et al., 2005) for low-temperature microbial dolomite was found inappropriate and therefore avoided for the calculation of water isotopic composition. The water rock ratio for dolomite lime mud ranged 0 to 0.1, whereas for other stromatolites it ranges from 2 to 50.9 based on the two end-member water oxygen isotope composition adopted in the present study (Fig. 5 and Table 1).

The clumped isotope study based on microbial carbonate by Thaler et al. (2020) commented on the higher temperature range observed in stromatolites as a product of the disequilibrium fractionation process experienced during the precipitation of biogenic carbonate. However, the apparent temperature evaluated from Δ_{47} values combined with carbonate $\delta^{18}O_{VPDB}$ according to them can provide an independent estimation of $\delta^{18}O_{VSMOW}$ value of water within analytical uncertainty (Thaler et al., 2020).

The range of clumped isotopic temperature observed in the primitive carbonate lime mud in the present study is colder than the Proterozoic seawater temperature and diagenetic temperature conditions reported from $d^{18}O$ of 1.9–2 Ga old Gunflint Chert (Marin et al., 2010) based on the Si^{30} record (Robert and Chaussidon, 2006) in chert of similar age. While $d^{18}O$ profiles in micro-quartz suggested temperature value of 37–52 °C for the precipitation of original silica in the Early Proterozoic Ocean (Marin et al., 2010), the Si^{30} isotope thermometer yielded a temperature value of ~25 °C for the Early Proterozoic Ocean (Robert and Chaussidon, 2006). The duration of deposition of Vempalle carbonates in the section (Rai et al., 2015), based on an upper age limit from intrusive sills (French et al., 2008) and intersecting dykes, is ~100 Ma. This possibly indicates the time duration for late phase diagenetic transformation of the original shallow water sediments by hydrothermal fluids with heavier isotopic values. This late phase diagenesis could be the reason for the reordering of clumped isotope composition in the overlying dolomites having stromatolite structure. The late-phase diagenetic alteration of oxygen isotopic composition in cherts (Sengupta and Pack, 2018; Liljestrand et al., 2020; Sengupta et al., 2020) from different Precambrian sedimentary basins also showed a similar tendency to register ^{17}O excess with progressive burial and associated precipitation. However, the low temperature and lighter oxygen isotopic compositions reported here for dolomite lime mud specimens in the Paleoproterozoic record is a unique observation (Kasting et al., 2006; Galili et al., 2019; Vérard and Veizer, 2019) suggesting retention of original sea water composition with minimal or limited transformation.

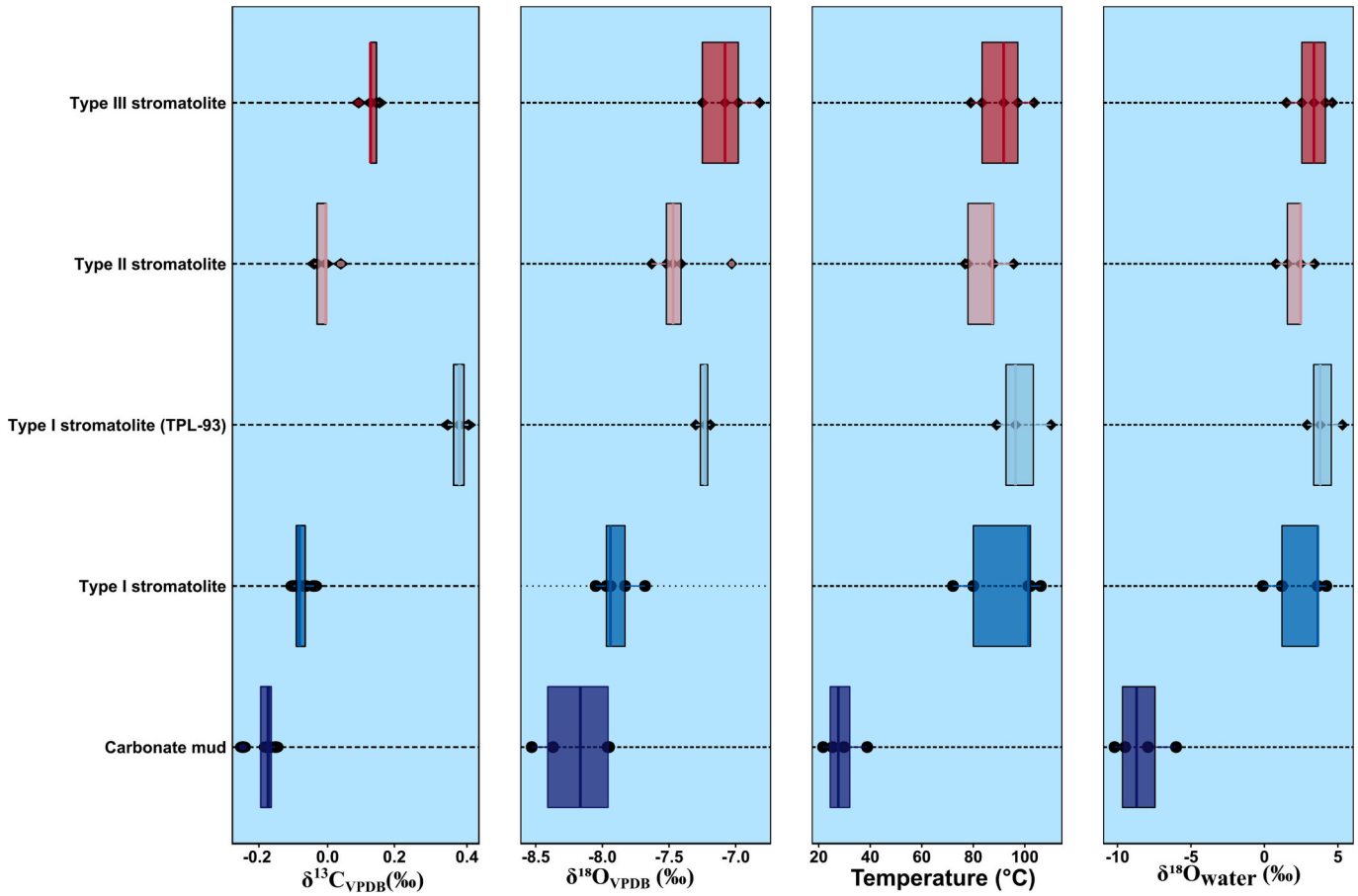

Fig. 3. Stratigraphic record showing the evolution of $\delta^{13}C_{VPDB}$ and δ^{18} O_{VPDB} clumped isotope-based temperature estimates for specific samples and equilibrium water isotopic composition (δ18 OVSMOW) measured in dolomite from lime mud, and type I, type II, and type III stromatolite units.

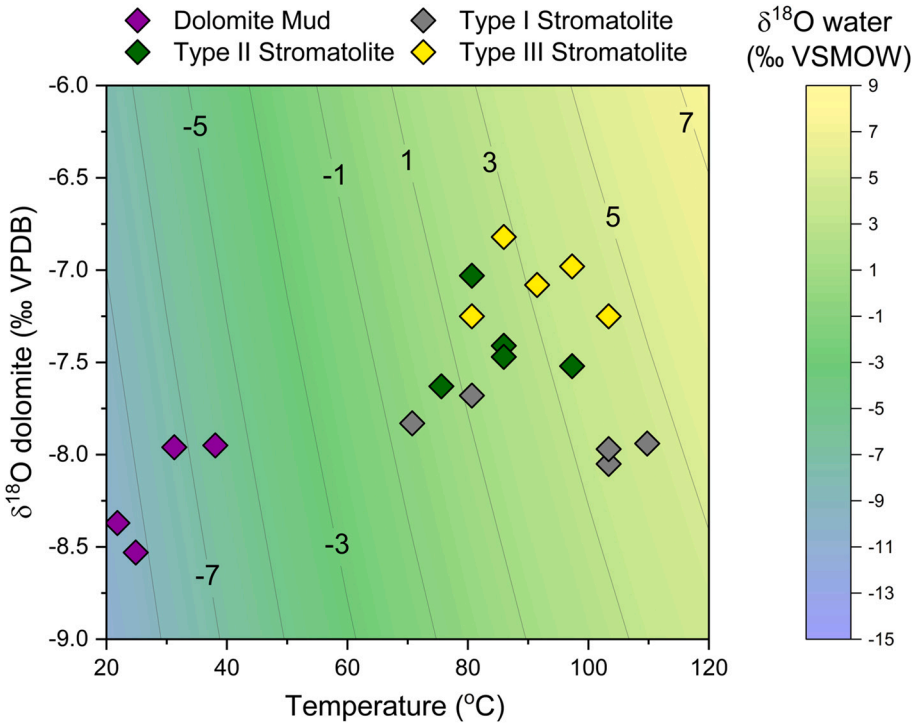

Fig. 4. Distribution of clumped isotope-based temperatures and δ^{18} O_{VPDB} of the dolomite mud and stromatolite samples. The secondary x-axis represents Δ47 values that were obtained by clumped isotope analysis. The thermometric equation for dolomite proposed by Müller et al. (2019) is used for temperature determination. Contours that define the water isotope composition (δ18 OVSMOW) of fluids were generated from the fractionation factor equation proposed for dolomite by Müller et al. (2019).

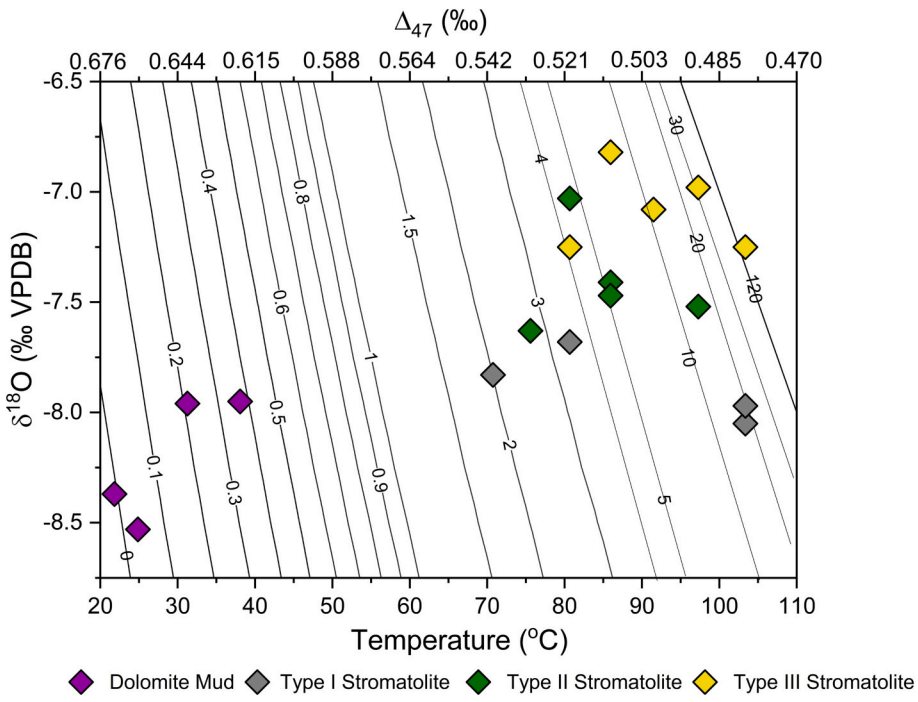

Fig. 5. Variation of clumped isotope temperature and δ18OVPDB values for dolomite mud and the three categories of stromatolites sampled. Secondary x-axis represents Δ47 values obtained by analysis and used for the evaluation of temperature using the thermometric equation for dolomite proposed by Müller et al. (2019). Contours represent the water-rock ratio or degree of water-rock interaction, assuming 4.74‰ as the heavier isotope value (hydrothermal or diagenetic source) reported from a stromatolite sample preserving an extreme temperature value (109.6 °C) denoting maximum hydrothermal fluid flux.

The ability of the surrounding chert layers encasing the lime mud to deter the process of transformation provides an ideal condition for preservation. Chert and micritic dolomite act as a barrier or impermeable lithology preventing water rock interaction during the process of burial diagenesis and hydrothermal fluid action.

5.3. Depositional conditions in the Paleoproterozoic rift basin

Consistent with previous paleomagnetic (Pradhan et al., 2010), sedimentological and geochemical inferences, Vempalle carbonates were precipitated in an equatorial sea with restricted connection with the open ocean These conditions favored deposition of microbially induced and inorganically precipitated dolomites on the carbonate ramp of an epicontinental sea (Paris and Donnadieu, 2012; Gilleaudeau and Kah, 2013) that developed during the early phase of rifting, and are characterized by lighter oxygen isotopic composition. Enhanced CO_2 levels (Charnay et al., 2013) in the atmosphere accelerated the continental weathering of basalt which was a primary basement lithology (Manikyamba et al., 2009), generating Mg ions in solution that contributed to the precipitation of early microbial dolomite lime mud and the overlying stromatolite layers.

The lighter oxygen isotopic composition (−9.94‰) established from the dolomite mud agrees with the compositional range inferred using the modelled data (Kasting et al., 2006; Jaffrés et al., 2007), which is based on continuous isotopic exchange as a result of weathering of volcanic rocks present in the greenstone belts. The emergence of spreading ridges with faster spreading rates in the Paleoproterozoic could have led to the lower seawater $\delta^{18}O$ values documented in this study. The $\delta^{18}O$ values of water estimated from the SIMS data on kerogen of Gunflint Chert (Tartèse et al., 2017) and iron oxides (goethite and hematite) (Galili et al., 2019) are comparable with the estimates in the present study. The $\delta^{18}O$ of the parent fluids responsible for the iron oxide precipitation, under the assumption of a constant temperature (15 ± 10 °C) yielded value of −7.5 ‰, closely resemble (heavier by 2.4 ‰) the value estimated in the present study (Galili et al., 2019). Early dolomite is quite common at this time. This could reflect the precipitation of aragonite sediment that was synsedimentarily replaced by dolomite in seawater with elevated Mg/Ca. In this case, the dolomite would be virtually primary and could reflect the depositional temperature (Galili et al., 2019) of shallow seawater around 1.88–2.0 Ga ago, providing a sea water signature which is lighter and in agreement with the $d^{18}O$ record in silica through time proposed more recently based on compilation of chert data through geological time (Tatzel et al., 2022).

Previous inferences based on rare earth element (REE) distribution in carbonates (Khelen et al., 2017; Banerjee et al., 2019) are consistent with our interpretation that positive Eu anomalies reported from the dolomitic layer reflect interaction with fluids from hydrothermal sources. The present study identified fluid of heavier isotopic composition which was either of mantle origin, or residual ocean water generated in a desiccated basin, and was responsible for the late phase precipitation of stromatolitic dolomite. The present study documents lighter $\delta^{18}Osw$ in sea water ~1.8–2 Ga and a cooler ocean, suitable for the proliferation of both microbial and algal life in these epicontinental seaways, as evident from the sedimentary record. Alternatively, the lighter isotopic imprint recorded in the precipitate may be similar to the oxygen isotope ($\delta^{18}O$) signature in the Late Proterozoic epicontinental sea rather than an open oceanwater signature, possibly resembling the paleoceanographic setting of a present-day epicontinental sea such as the Black Sea which experienced variable connection with the Mediterranean Sea during the last few million-years (Badertscher et al., 2011). The lower isotopic composition measured in Vempalle dolomite lime mud, when compared with present-day epicontinental seawater near the equator, is characterized by heavier composition (modern day value of meteoric water −2 to −5 ‰ from Cauquoin et al., 2019). Ocean water isotopic value is strongly linked to excess freshwater input, and will make the open ocean water isotopic value lighter than that of the present day.

6. Conclusion

This study documents for the first time a systematic variation in clumped isotope-based temperature estimates from dolomitic lime mud overlain by three different stromatolites with distinct morphotypes in the sedimentary succession of the Paleoproterozoic Vempalle Formation in southern India. These dolomites consist of two different types that registered the isotopic signatures of two distinct thermal conditions: dolomitic lime-mud preserving the original signature of seawater, and

overlying stromatolites preserving the signatures of differing degrees of late phase hydrothermal alteration. This study suggests that the dolomitic lime-mud preserves the signatures of Paleoproterozoic seawater temperature which are significantly lower than previous estimates. The temperature value of 21.8 ± 2 °C (Table 1 and Fig. 1) and oxygen isotope composition −9.94 ± 0.02‰ for the seawater match expectations for biogenic precipitation. In contrast, stromatolites of varied morphology and texture experienced transformation or reordering of clumped isotopic composition at higher temperatures (70.8–109.8 °C). Type III stromatolite collected from the sequence represents a dolomite that has experienced the maximum degree of hydrothermal activity with involvement of water having isotopic composition of 4.45‰. The isotopic data from pristine dolomite mud denote the water composition and temperature of a Paleoproterozoic equatorial shallow epicontinental sea, unknown till now.

Declaration of Competing Interest

None.

Data availability

200

Acknowledgements

This work was supported by a research fellowship from the Council of Scientific and Industrial Research-University Grants Commission, India (Sr.No. 1061620567, Ref. No: 19/06/2016(i)EU-V) to SB, and by departmental support generated through a generous award from the Ministry of Earth Sciences, India (Sanction: MoES/ATMOS/PP-IX/09). We thank Ramesh Chandra Mallick and Sanyukta Ghosh (Department of Physics, Indian Institute of Science, Bangalore) for XRD analyses of the carbonate samples analyzed in this study. We thank reviewers Daniel Herwartz and Swapan Sahoo for comments and suggestions which have improved the quality of our paper. Special gratitude to R. Srinivasan (Divecha Centre for Climate Change, IISc), who provided all input for conducting our fieldwork.

Appendix A. Supplementary data

Supplementary data to this article can be found online at https://doi.org/10.1016/j.chemgeo.2023.121356.

References

Anand, M., Gibson, S.A., Subbarao, K.V., Kelley, S.P., Dickin, A.P., 2003. Early Proterozoic Melt Generation Processes beneath the Intra-cratonic Cuddapah Basin, Southern India, 44, pp. 2139–2171. https://doi.org/10.1093/petrology/egg073.

Badertscher, S., Fleitmann, D., Cheng, H., Edwards, R.L., Göktürk, O.M., Zumbühl, A., Leuenberger, M., Tüysüz, O., 2011. Pleistocene water intrusions from the Mediterranean and Caspian seas into the Black Sea. Nat. Geosci. 4, 236–239. https://doi.org/10.1038/ngeo1106.

Banerjee, A., Słowakiewicz, M., Majumder, T., Khan, S., Patranabis-Deb, S., Tucker, M.E., Saha, D., 2019. A Palaeoproterozoic dolomite (Vempalle Formation, Cuddapah Basin, India) showing Phanerozoic-type dolomitisation. Precambrian Res. 328, 9–26. https://doi.org/10.1016/j.precamres.2019.04.013.

Bonifacie, M., et al., 2017. Calibration of the dolomite clumped isotope thermometer from 25 to 350 °C, and implications for a universal calibration for all (Ca, Mg, Fe) CO3 carbonates. Geochim. Cosmochim. Acta 200, 255–279. https://doi.org/10.1016/j.gca.2016.11.028.

Cauquoin, Alexandre, Werner, Martin, Lohmann, Gerrit, 2019. Water isotopes - climate relationships for the mid-Holocene and preindustrial period simulated with an isotope-enabled version of MPI-ESM. Clim. Past 15 (6), 1913–1937. https://doi.org/10.5194/cp-15-1913-2019.

Chakrabarti, G., Shome, D., Kumar, S., Stephens, G.M., Kah, L.C., 2014. Carbonate platform development in a Paleoproterozoic extensional basin, Vempalle formation, Cuddapah Basin, India. J. Asian Earth Sci. 91, 263–279. https://doi.org/10.1016/j.jseaes.2013.09.028.

Charnay, B., Forget, F., Wordsworth, R., Leconte, J., Millour, E., Codron, F., Spiga, A., 2013. Exploring the faint young Sun problem and the possible climates of the Archean Earth with a 3-D GCM. J. Geophys. Res.-Atmos. 118, 10,414–10,431. https://doi.org/10.1002/jgrd.50808.

Daëron, M., Blamart, D., Peral, M., Affek, H.P., 2016. Absolute isotopic abundance ratios and the accuracy of Δ47 measurements. Chem. Geol. 442, 83–96. https://doi.org/10.1016/j.chemgeo.2016.08.014.

Dennis, K.J., Affek, H.P., Passey, B.H., Schrag, D.P., Eiler, J.M., 2011. Defining an absolute reference frame for "clumped" isotope studies of CO2. Geochim. Cosmochim. Acta 75, 7117–7131. https://doi.org/10.1016/j.gca.2011.09.025.

Fosu, B.R., Ghosh, P., Mishra, D., Banerjee, Y., Prasanna, K., Sarkar, A., 2019. Acid digestion of carbonates using break seal method for clumped isotope analysis. Rapid Commun. Mass Spectrom. 33, 203–214. https://doi.org/10.1002/rcm.8304.

Frantz, C.M., Petryshyn, V.A., Marenco, P.J., Tripati, A., Berelson, W.M., Corsetti, F.A., 2014. Dramatic local environmental change during the early eocene climatic optimum detected using high resolution chemical analyses of Green River Formation stromatolites. Palaeogeogr. Palaeoclimatol. Palaeoecol. 405, 1–15. https://doi.org/10.1016/j.palaeo.2014.04.001.

French, J.E., Heaman, L.M., Chacko, T., Srivastava, R.K., 2008. 1891-1883 Ma Southern Bastar-Cuddapah mafic igneous events, India: a newly recognized large igneous province. Precambrian Res. 160, 308–322. https://doi.org/10.1016/j.precamres.2007.08.005.

Galili, N., et al., 2019. The geologic history of seawater oxygen isotopes from marine iron oxides. Science 365, 469–473. https://doi.org/10.1126/science.aaw9247.

Ghosh, P., Adkins, J., Affek, H., Balta, B., Guo, W., Schauble, E.A., Schrag, D., Eiler, J.M., 2006. 13C-18O bonds in carbonate minerals: A new kind of paleothermometer. Geochim. Cosmochim. Acta 70, 1439–1456. https://doi.org/10.1016/j.gca.2005.11.014.

Ghosh, P., Patecki, M., Rothe, M., Brand, W.A., 2005. Calcite-CO_2 mixed into CO_2-free air: A new CO_2-in-air stable isotope reference material for the VPDB scale. Rapid Commun. Mass Spectrom. 19, 1097–1119.

Gilleaudeau, G.J., Kah, L.C., 2013. Carbon isotope records in a Mesoproterozoic epicratonic sea: Carbon cycling in a low-oxygen world. Precambrian Res. 228, 85–101. https://doi.org/10.1016/j.precamres.2013.01.006.

Horita, J., 2014. Oxygen and carbon isotope fractionation in the system dolomite-water-CO2 to elevated temperatures. Geochim. Cosmochim. Acta 129, 111–124. https://doi.org/10.1016/j.gca.2013.12.027.

Jaffrés, J.B.D., Shields, G.A., Wallmann, K., 2007. The oxygen isotope evolution of seawater: a critical review of a long-standing controversy and an improved geological water cycle model for the past 3.4 billion years. Earth Sci. Rev. 83, 83–122. https://doi.org/10.1016/j.earscirev.2007.04.002.

Kasting, J.F., Howard, M.T., Wallmann, K., Veizer, J., Shields, G., Jaffrés, J., 2006. Paleoclimates, ocean depth, and the oxygen isotopic composition of seawater. Earth Planet. Sci. Lett. 252, 82–93. https://doi.org/10.1016/j.epsl.2006.09.029.

Khelen, A.C., Manikyamba, C., Ganguly, S., Singh, T.D., Subramanyam, K.S.V., Ahmad, S. M., Reddy, M.R., 2017. Geochemical and stable isotope signatures of Proterozoic stromatolitic carbonates from the Vempalle and Tadpatri Formations, Cuddapah Supergroup, India: Implications on paleoenvironment and depositional conditions. Precambrian Res. 298, 365–384. https://doi.org/10.1016/j.precamres.2017.05.021.

Liljestrand, F.L., Knoll, A.H., Tosca, N.J., Cohen, P.A., Macdonald, F.A., Peng, Y., Johnston, D.T., 2020. The triple oxygen isotope composition of Precambrian chert. Earth Planet. Sci. Lett. 537, 116167 https://doi.org/10.1016/j.epsl.2020.116167.

Manikyamba, C., Kerrich, R., Khanna, T.C., Satyanarayanan, M., Krishna, A.K., 2009. Enriched and depleted arc basalts, with Mg-andesites and adakites: a potential paired arc-back-arc of the 2.6 Ga Hutti greenstone terrane, India. Geochim. Cosmochim. Acta 73, 1711–1736. https://doi.org/10.1016/j.gca.2008.12.020.

Marin, J., Chaussidon, M., Robert, F., 2010. Microscale oxygen isotope variations in 1.9 Ga Gunflint cherts: Assessments of diagenesis effects and implications for oceanic paleotemperature reconstructions. Geochim. Cosmochim. Acta 74, 116–130. https://doi.org/10.1016/j.gca.2009.09.016.

Müller, I.A., Rodriguez-Blanco, J.D., Storck, J.C., do Nascimento, G.S., Bontognali, T.R. R., Vasconcelos, C., Benning, L.G., Bernasconi, S.M., 2019. Calibration of the oxygen and clumped isotope thermometers for (proto-)dolomite based on synthetic and natural carbonates. Chem. Geol. 525, 1–17. https://doi.org/10.1016/j.chemgeo.2019.07.014.

Panja, M., Chakrabarti, G., Shome, D., 2019. Earthquake induced soft sediment deformation structures in the Paleoproterozoic Vempalle Formation (Cuddapah basin, India). Carbonates Evaporites 34, 491–505. https://doi.org/10.1007/s13146-017-0412-z.

Paris, G., Donnadieu, Y., 2012. Modeling the consequences on late Triassic environment of intense pulse-like degassing during the Central Atlantic Magmatic Province using the GEOCLIM model. Clim. Past Discuss. 8, 2075–2110. https://doi.org/10.5194/cpd-8-2075-2012.

Patranabis-Deb, S., Majumder, T., Khan, S., 2018. Lifestyles of the palaeoproterozoic stromatolite builders in the Vempalle Sea, Cuddapah Basin, India. J. Asian Earth Sci. 157, 360–370. https://doi.org/10.1016/j.jseaes.2017.08.022.

Petryshyn, V.A., Lim, D., Laval, B.L., Brady, A., Slater, G., Tripati, A.K., 2015. Reconstruction of limnology and microbialite formation conditions from carbonate clumped isotope thermometry. Geobiology 13, 53–67. https://doi.org/10.1111/gbi.12121.

Pradhan, V.R., Meert, J.G., Pandit, M.K., Kamenov, G., Gregory, L.C., Malone, S.J., 2010. India's changing place in global Proterozoic reconstructions: a review of geochronologic constraints and paleomagnetic poles from the Dharwar, Bundelkhand and Marwar cratons. J. Geodyn. 50, 224–242. https://doi.org/10.1016/j.jog.2009.11.008.

Pramanik, C., Ghosh, P., Banerjee, S., Liang, M., 2020. Ab initio quantum chemical studies of isotopic fractionation during acid digestion reaction of dolomite for

clumped isotope application. Rapid Commun. Mass Spectrom. 34, 1–12. https://doi.org/10.1002/rcm.8926.

Rai, A.K., Pandey, U.K., Zakaulla, S., Parihar, P.S., 2015. New 1.9-2.0 Ga, Pb-Pb (PbSL), age of dolomites from Vempalle Formation, lower Cuddapah Supergroup, Eastern Dharwar craton, India. J. Geol. Soc. India 86, 131–136. https://doi.org/10.1007/s12594-015-0292-6.

Rangarajan, R., Pathak, P., Banerjee, S., Ghosh, P., 2021. Floating boat method for carbonate stable isotopic ratio determination in a GasBench II peripheral. Rapid Commun. Mass Spectrom. 35, 0–2. https://doi.org/10.1002/rcm.9115.

Riding, R., Sharma, M., 1998. Late Palaeoproterozoic (~1800-1600 Ma) stromatolites, Cuddapah Basin, southern India: cyanobacterial or other bacterial microfabrics? Precambrian Res. 92, 21–35. https://doi.org/10.1016/S0301-9268(98)00065-5.

Robert, F., Chaussidon, M., 2006. A palaeotemperature curve for the Precambrian oceans based on silicon isotopes in cherts. Nature 443, 969–972.

Sengupta, S., Pack, A., 2018. Triple oxygen isotope mass balance for the Earth's oceans with application to Archean cherts. Chem. Geol. 495, 18–26. https://doi.org/10.1016/j.chemgeo.2018.07.012.

Sengupta, S., Peters, S.T.M., Reitner, J., Duda, J.P., Pack, A., 2020. Triple oxygen isotopes of cherts through time. Chem. Geol. 554, 119789 https://doi.org/10.1016/j.chemgeo.2020.119789.

Singh, T.D., et al., 2018. Mantle heterogeneity, plume-lithosphere interaction at rift controlled ocean-continent transition zone: Evidence from trace-PGE geochemistry of Vempalle flows, Cuddapah Basin, India. Geosci. Front. https://doi.org/10.1016/j.gsf.2017.12.01.

Tartèse, R., Chaussidon, M., Gurenko, A., Delarue, F., Robert, F., 2017. Warm Archean oceans reconstructed from oxygen isotope composition of early-life remnants. Geochem. Perspect. Lett. 3, 55–65. https://doi.org/10.7185/geochemlet.1706.

Tatzel, M., Frings, P.J., Oelze, M., Herwartze, D., Lünsdorfa, N.K., Wiedenbeck, M., 2022. Chert oxygen isotope ratios are driven by Earth's thermal evolution. Proc. Natl. Acad. Sci. 119 (51), 3–7.

Thaler, C., Millo, C., Ader, M., Chaduteau, C., 2016. Disequilibrium & δ18O values in microbial carbonates as a tracer of metabolic production of dissolved inorganic carbon. Geochim. Cosmochim. Acta. https://doi.org/10.1016/j.gca.2016.10.051.

Thaler, C., Katz, A., Bonifacie, M., Ménez, B., Ader, M., 2020. Oxygen isotope composition of waters recorded in carbonates in strong clumped and oxygen isotopic disequilibrium. Biogeosciences 1731–1744. https://doi.org/10.5194/bg-17-1731-2020.

Vasconcelos, C., McKenzie, J.A., Warthmann, R., Bernasconi, S.M., 2005. Calibration of the $\delta^{18}O$ paleothermometer for dolomite precipitated in microbial cultures and natural environments. Geology 33, 317–320. https://doi.org/10.1130/G20992.1.

Vérard, C., Veizer, J., 2019. On plate tectonics and ocean temperatures. Geology 47, 882–885. https://doi.org/10.1130/G46376.1.